Electronic Supplementary Information for:

Protonation and electrochemical reduction of rhodium- and iridium-dinitrogen complexes in organic solution

G. P. Connor,[a] N. Lease,[b] A. Casuras,[b] A. S. Goldman,*[b] P. L Holland*[a] and J. M. Mayer*[a]

[a]*Department of Chemistry, Yale University, New Haven, Connecticut 06511, USA*
[b]*Department of Chemistry and Chemical Biology, Rutgers, The State University of New Jersey, New Brunswick, New Jersey 08903, USA*

TABLE OF CONTENTS:

Supplementary Data and Spectra:

Fig. S1: FTIR spectrum of **1**

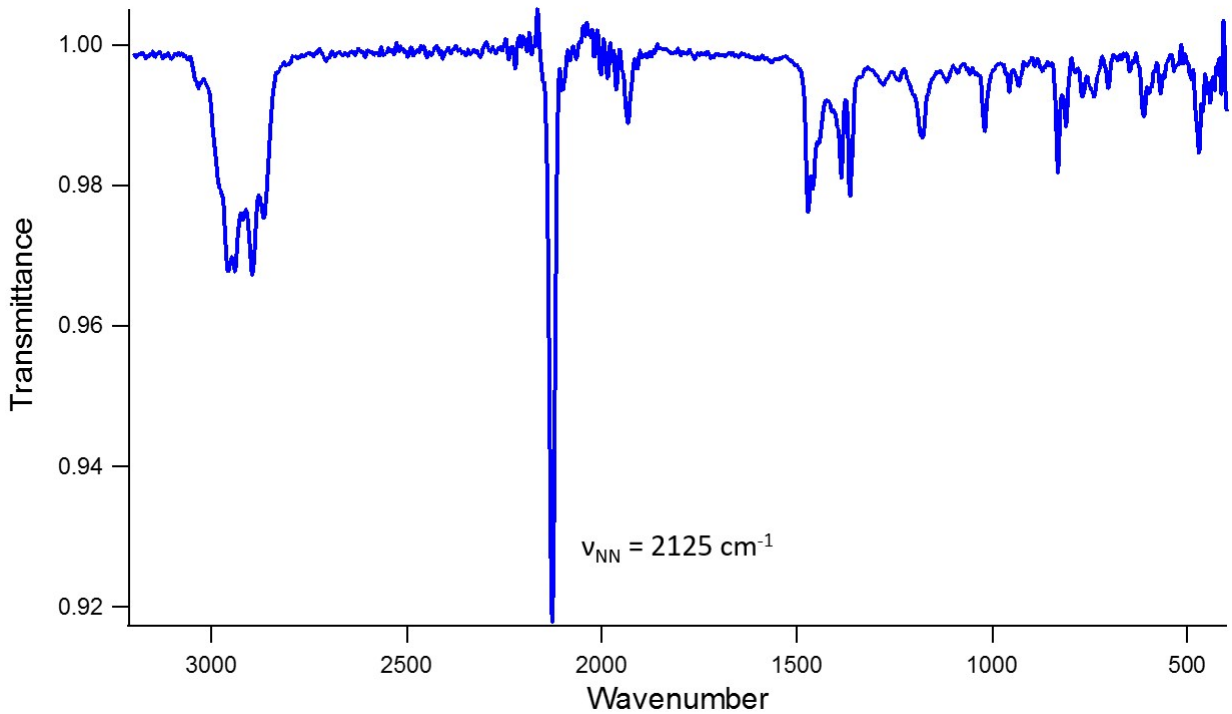

Fig. S2: FTIR spectrum of **2**

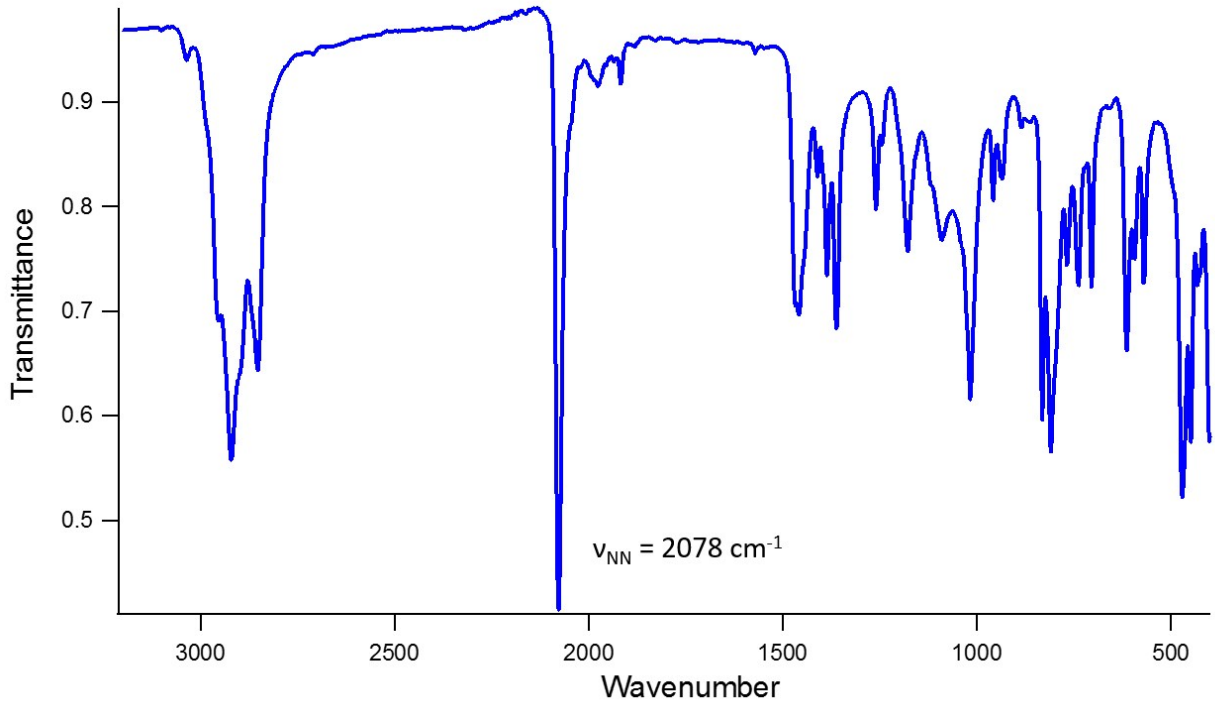

Fig. S3: ^{1}H NMR spectra showing protonation of **1** with TFA in THF-d_8

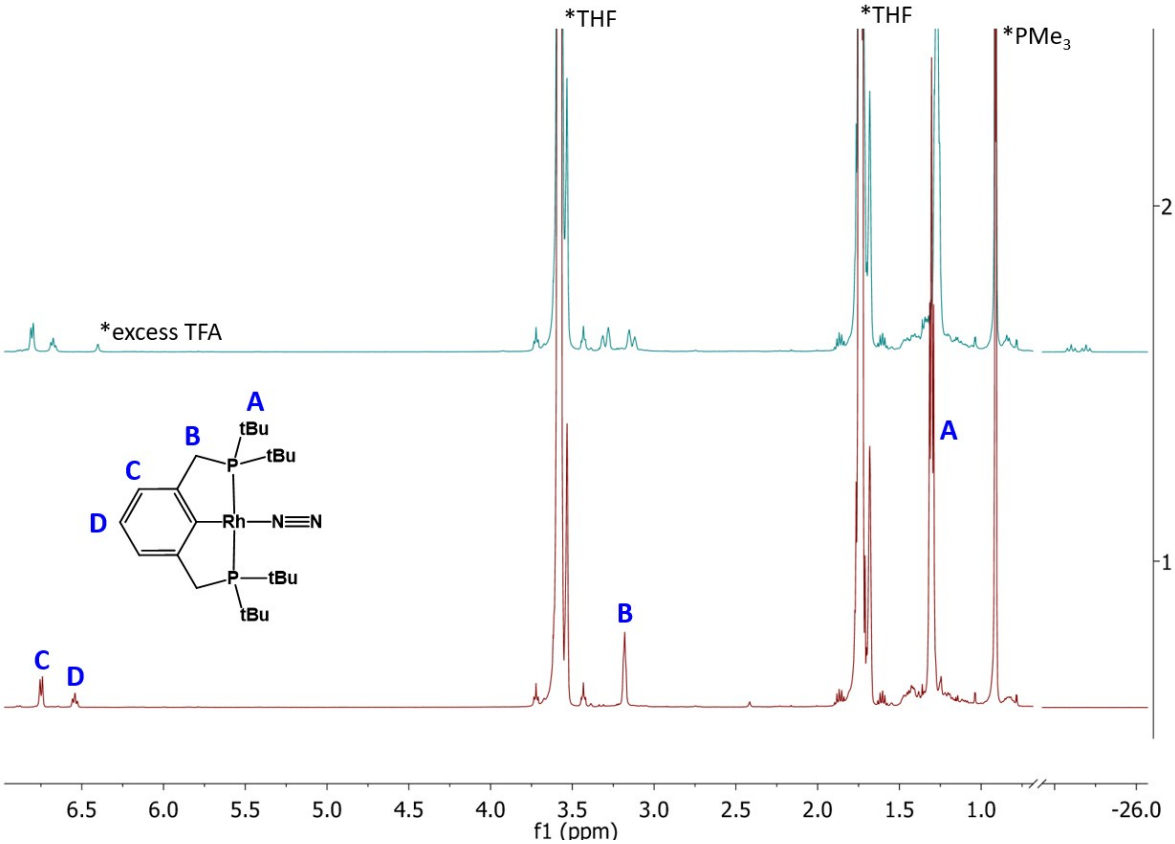

Bottom (1, maroon): 1.7 mg **1** (3.2 µmol) in THF-d_8. ^{1}H NMR (500 MHz, THF-d_8): δ = 6.80 (d, $^{3}J_{H,H}$ = 7.3 Hz, 2H, *m*-Ph), 6.59 (t, $^{3}J_{H,H}$ = 7.3 Hz, 1H, *p*-Ph), 3.23 (m, 4H, CH_2), 1.35 (m, $^{2}J_{P,H}$ = 6.2 Hz, 36H, C(CH_3)$_3$). *Top (2, teal):* 1.7 mg **1** in THF-d_8 with 1.1 eq. TFA added. ^{1}H NMR (500 MHz, THF-d_8, **1a**): δ = 6.85 (d, $^{3}J_{H,H}$ = 7.3 Hz, 2H, *m*-Ph), 6.72 (t, $^{3}J_{H,H}$ = 7.3 Hz, 1H, *p*-Ph), 3.38 – 3.13 (m, 4H, CH_2), 1.32 (m, $^{2}J_{P,H}$ = 6.4 Hz, 36H, C(CH_3)$_3$), -25.60 (dt, $^{1}J_{Rh,H}$ = 45.4, $^{2}J_{P,H}$ = 11.8 Hz, 1H, Rh-*H*). The spectrum describes a diamagnetic complex, and the loss of C_{2v} symmetry is evident from splitting of methylene and ^{t}Bu resonances. A hydride peak is visible at -25.60 ppm. The PMe_3 peak is from the internal standard in a capillary tube.

Fig. S4: $^{31}P\{^{1}H\}$ NMR spectra showing protonation of **1** with TFA in THF-d_8

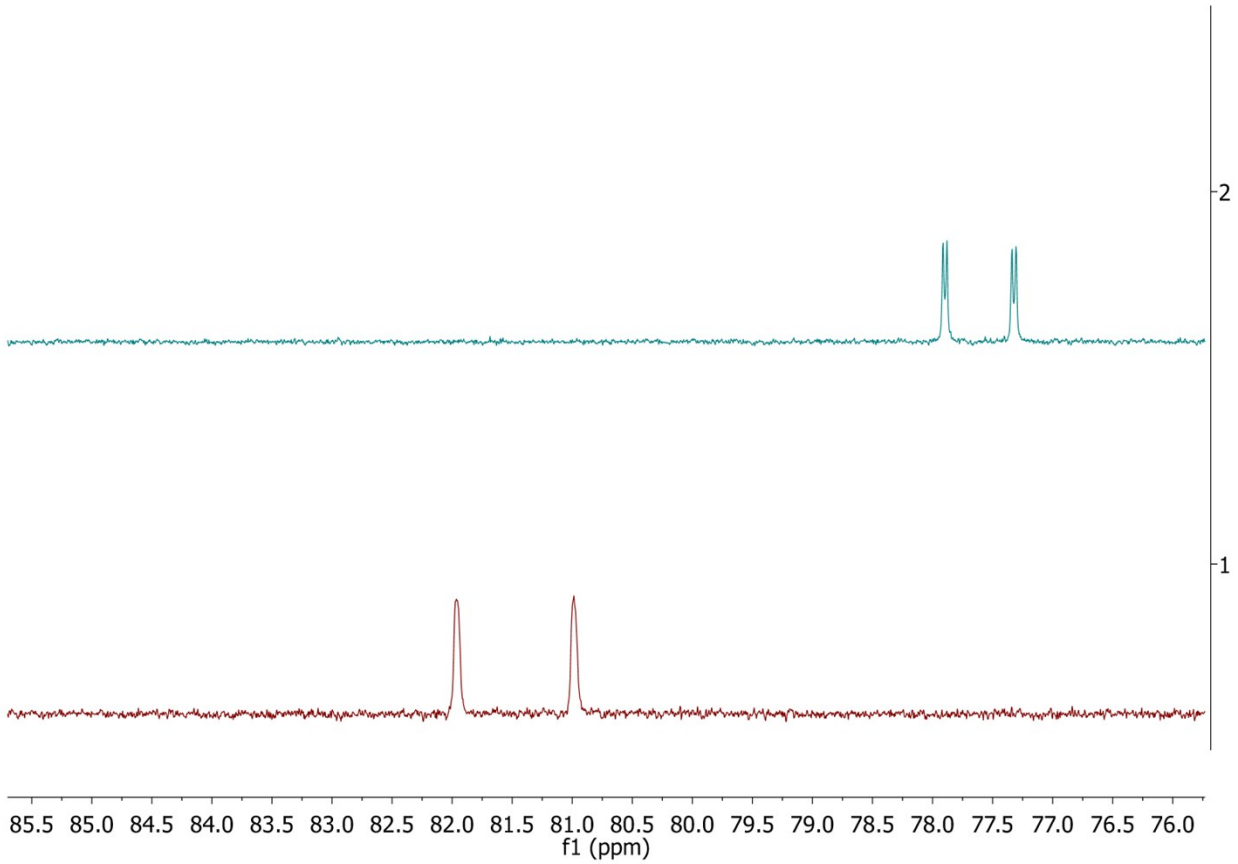

Bottom (1, maroon): 1.7 mg **1** (3.2 µmol) in THF-d_8. $^{31}P\{^{1}H\}$ NMR (162 MHz, THF-d_8): δ = 81.48 (d, $^{1}J_{P,Rh}$ = 158.2 Hz). *Top (2, teal):* 1.7 mg **1** in THF-d_8 with 1.1 eq. TFA added. $^{31}P\{^{1}H\}$ NMR (202 MHz, THF-d_8): δ = 77.61 (dd, $^{1}J_{P,Rh}$ = 116.4 Hz, $^{2}J_{P,H}$ = 6.8 Hz, **1a**). Referenced to PMe_3 in a capillary tube.

Fig. S5: ^{19}F NMR spectra showing protonation of **1** with TFA in THF-d_8

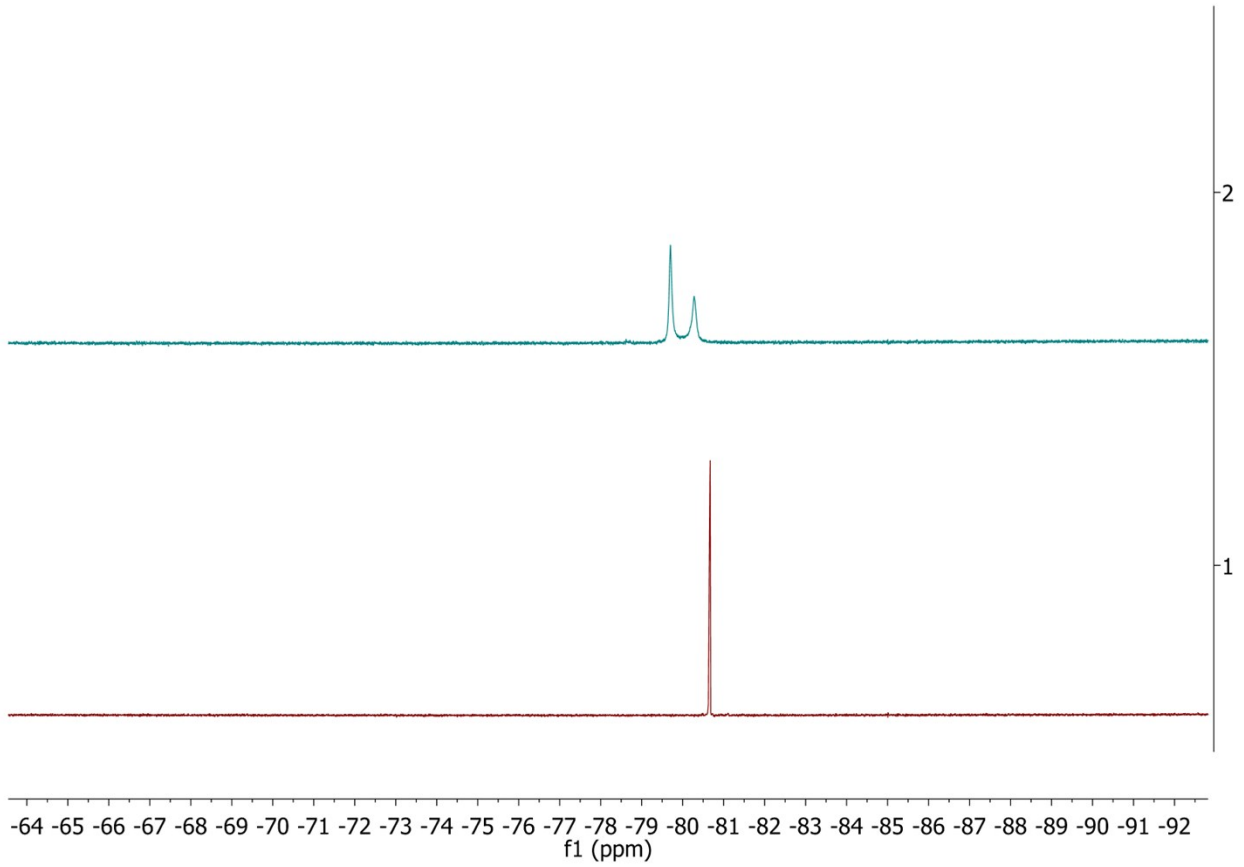

Bottom (1, maroon): 3.0 µmol TFA in THF-d_8. ^{19}F NMR (470 MHz, THF-d_8): δ = -80.67 (s). *Top (2, teal):* 3.0 µmol TFA with 1.4 mg **1** (2.7 µmol, 0.9 eq.) added in THF-d_8. ^{19}F NMR (470 MHz, THF-d_8): δ = -79.70 (s), -80.28 (br. s).

Fig. S6: $^{31}P\{^{1}H\}$ NMR spectra showing protonation of **1** with *p*CAH-BF_4 and deprotonation of **1b** with DBU under N_2

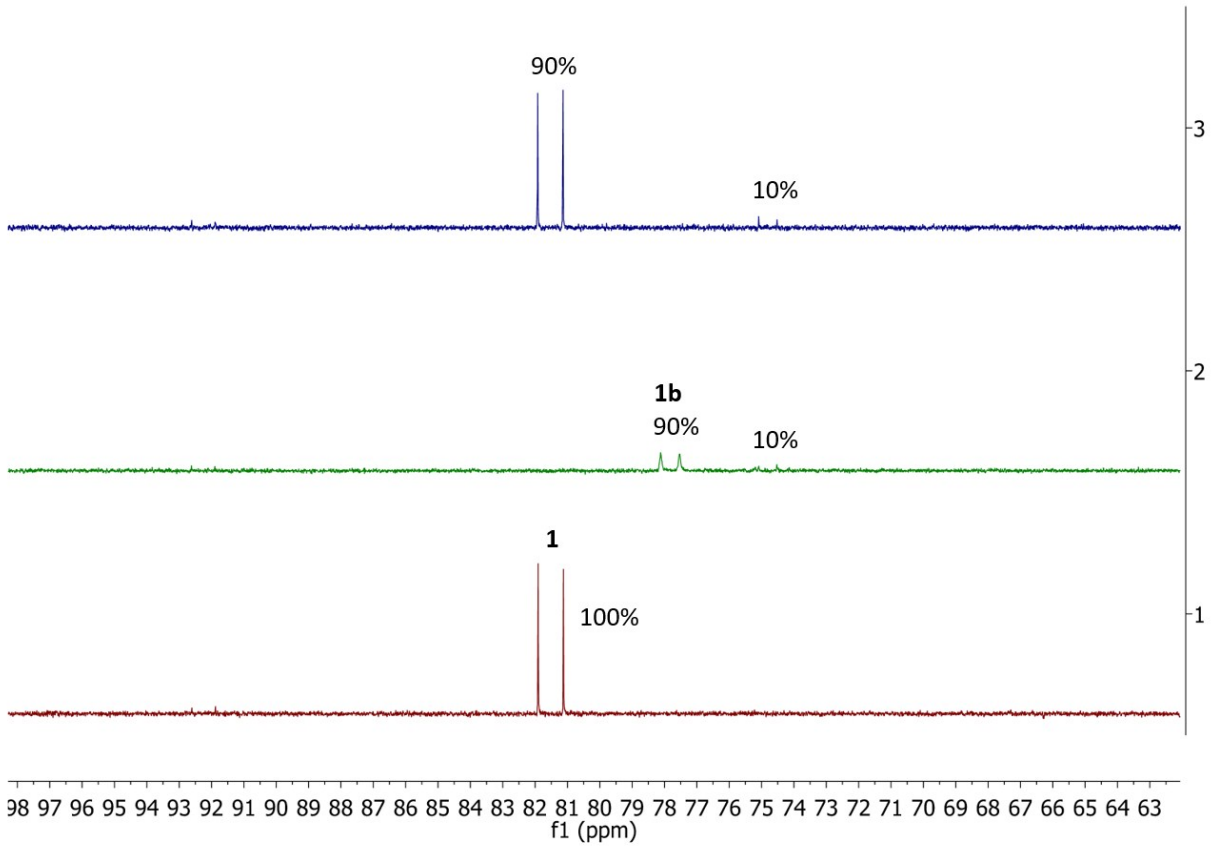

Bottom (1, maroon): 1.2 mg **1** (2.3 µmol) in THF-d_8 under N_2. $^{31}P\{^{1}H\}$ NMR (202 MHz, THF-d_8): δ = 81.52 (d, $^{1}J_{P,Rh}$ = 157.9 Hz, 100%). *Middle (2, green)*: 1.2 mg **1** with 1 eq. *p*CAH-BF_4 in THF-d_8 under N_2. $^{31}P\{^{1}H\}$ NMR (202 MHz, THF-d_8): δ = 77.83 (d, $^{1}J_{P,Rh}$ = 117.4 Hz, 90%, **1b**), 74.81 (d, $^{1}J_{P,Rh}$ = 112.7 Hz, 10%). *Top (3, blue)*: 1.2 mg **1** with 1 eq. *p*CAH-BF_4 and 1.1 eq. DBU in THF-d_8 under N_2. $^{31}P\{^{1}H\}$ NMR (202 MHz, THF-d_8): δ = 81.53 (d, $^{1}J_{P,Rh}$ = 157.9 Hz, 90%), 74.80 (d, $^{1}J_{P,Rh}$ = 115.2 Hz, 10%). Protonation of **1** with *p*CAH-BF_4 under N_2 gives **1b**, and subsequent addition of DBU reforms complex **1** in 90% yield. Integrations are referenced to an internal standard of PMe_3 in a capillary tube, and yields are rounded to one significant figure.

Fig. S7: $^{31}P\{^{1}H\}$ NMR spectra showing protonation of **1** with *p*CAH-BF_4 and deprotonation of **1b** with DBU under Ar

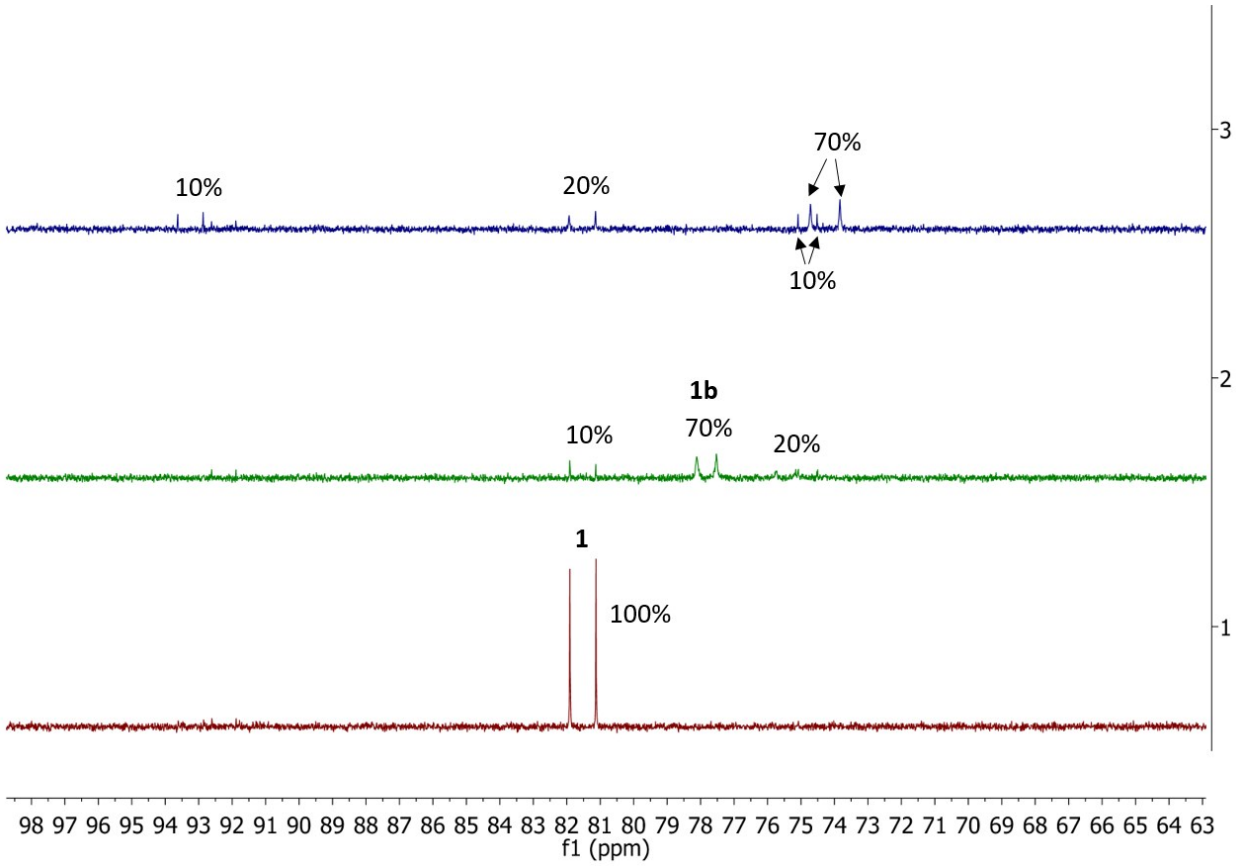

Bottom (1, maroon): 1.3 mg **1** (2.5 µmol) in THF-d_8 under Ar. $^{31}P\{^{1}H\}$ NMR (202 MHz, THF-d_8): δ = 81.52 (d, $^{1}J_{P,Rh}$ = 158.0 Hz, 100%). *Middle (2, green):* 1.3 mg **1** with 1 eq. *p*CAH-BF_4 in THF-d_8 under Ar. $^{31}P\{^{1}H\}$ NMR (202 MHz, THF-d_8): δ = 81.52 (d, $^{1}J_{P,Rh}$ = 157.7 Hz, 10%), 77.82 (br. d, $^{1}J_{P,Rh}$ = 121.2 Hz, 70%, **1b**), 75.45 (d, $^{1}J_{P,Rh}$ = 120.6 Hz, 20%). *Top (3, blue):* 1.3 mg **1** with 1 eq. *p*CAH-BF_4 and 1.1 eq. DBU in THF-d_8 under Ar. $^{31}P\{^{1}H\}$ NMR (202 MHz, THF-d_8): δ = 93.25 (d, $^{1}J_{P,Rh}$ = 154.0 Hz, 10%), 81.54 (d, $^{1}J_{P,Rh}$ = 159.7 Hz, 20%), 74.80 (d, $^{1}J_{P,Rh}$ = 115.0 Hz, 10%), 74.28 (d, $^{1}J_{P,Rh}$ = 178.3 Hz, 70%). Integrations are referenced to an internal standard of PMe_3 in a capillary tube, and yields are rounded to one significant figure.

Fig. S8: VT ^{1}H NMR spectra upon protonation of **2** with DMAH-BF_4 to form **2a**

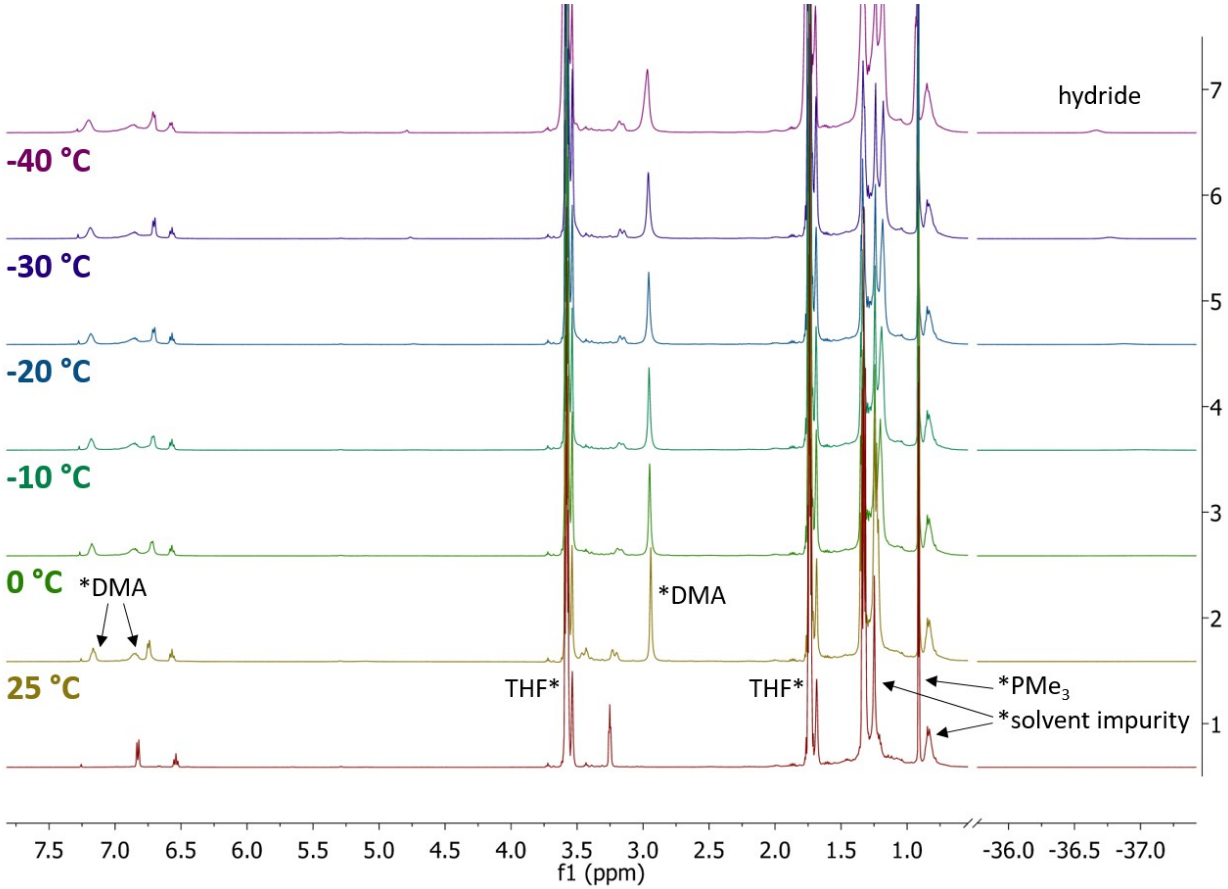

Bottom (1, maroon): 3.4 mg **2** (5.5 µmol) in THF-d_8. ^{1}H NMR (500 MHz, THF-d_8, **2**): δ = 6.83 (d, $^3J_{H,H}$ = 7.4 Hz, 2H, *m*-Ph), 6.54 (t, $^3J_{H,H}$ = 7.4 Hz, 1H, *p*-Ph), 3.25 (m, 4H, CH_2), 1.33 (m, $^2J_{P,H}$ = 6.4 Hz, 36H, C(CH_3)$_3$). *Second to bottom (2, gold):* 3.4 mg **2** (5.5 µmol) with 1 eq. DMAH-BF_4 in THF-d_8 at 25 °C. ^{1}H NMR (500 MHz, THF-d_8, **2a**) δ = 6.75 (d, $^3J_{H,H}$ = 7.5 Hz, 2H, *m*-Ph), 6.57 (t, $^3J_{H,H}$ = 7.5 Hz, 1H, *p*-Ph), 3.50 – 3.15 (m, 4H, CH_2), 1.34 (m, $^2J_{P,H}$ = 6.7 Hz, 18H, C(CH_3)$_3$), 1.27 – 1.15 (m, 18H, C(CH_3)$_3$). The spectrum describes a diamagnetic complex, and the loss of C_{2v} symmetry is evident from splitting of methylene and ^{t}Bu resonances; however, no hydride resonance is resolved at ambient temperature. *Third from bottom and upwards (3-7, green through plum)*: 3.4 mg **2** (5.5 µmol) with 1 eq. DMAH-BF_4 in THF-d_8 at various temperatures. A hydride resonance resolves at low temperatures and is visible at -40 °C at δ = -36.7 (br. s, 1H, Ir-*H*).

Fig. S9: VT $^{31}P\{^{1}H\}$ NMR spectra upon protonation of **2** with DMAH-BF_4 to form **2a**

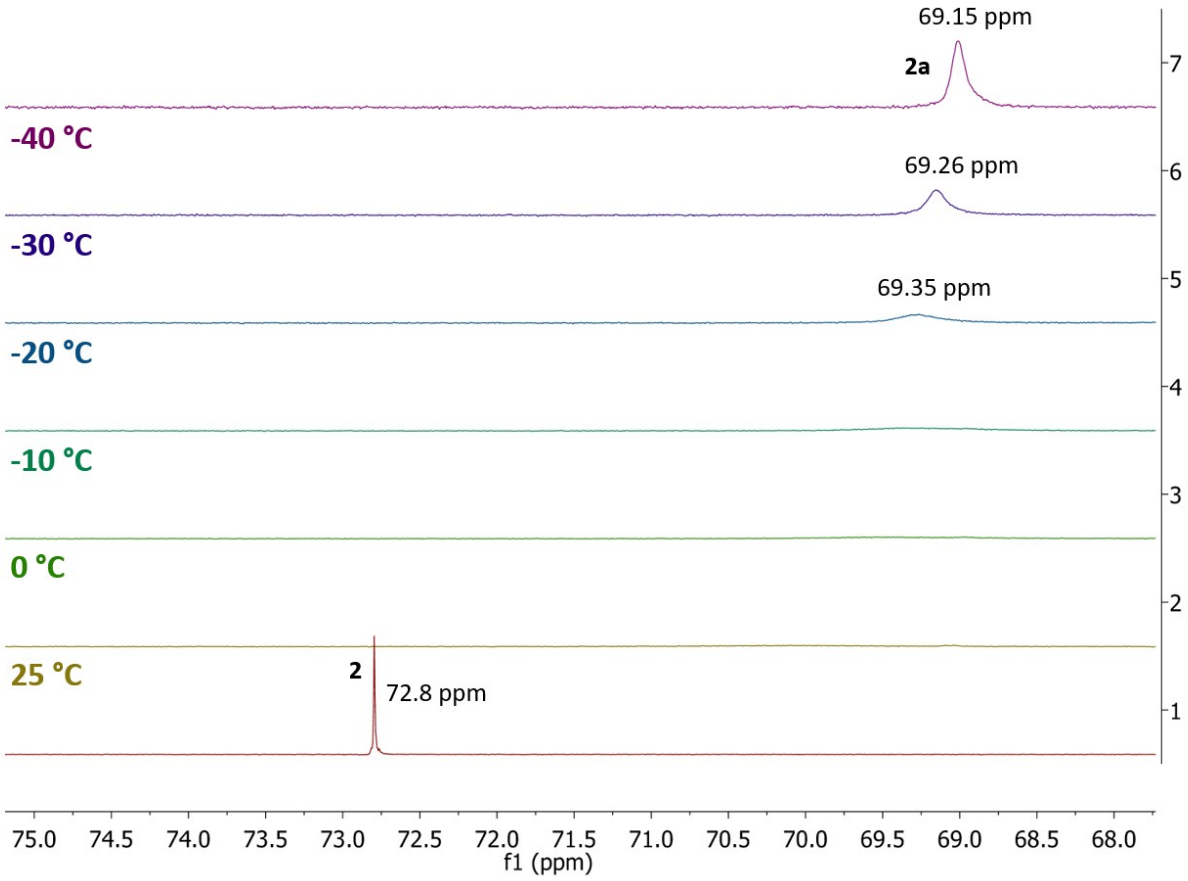

Bottom (1, maroon): 3.4 mg **2** (5.5 µmol) in THF-d_8. $^{31}P\{^{1}H\}$ NMR (202 MHz, THF-d_8, **2**): δ = 72.80 (s). *Second to bottom (2, gold):* 3.4 mg **2** (5.5 µmol) with 1 eq. DMAH-BF_4 in THF-d_8 at 25 °C. No phosphorus resonance is visible for the diamagnetic complex described in the corresponding ^{1}H NMR spectrum (see Fig. S8). *Third from bottom and upwards (3-7, green through plum)*: 3.4 mg **2** (5.5 µmol) with 1 eq. DMAH-BF_4 in THF-d_8 at various temperatures. A phosphorus resonance resolves at low temperatures and is visible at -40 °C at δ = 69.15 (br. s).

Fig. S10: $^{31}P\{^{1}H\}$ NMR spectra showing deprotonation of **2a** with DBU under N_2

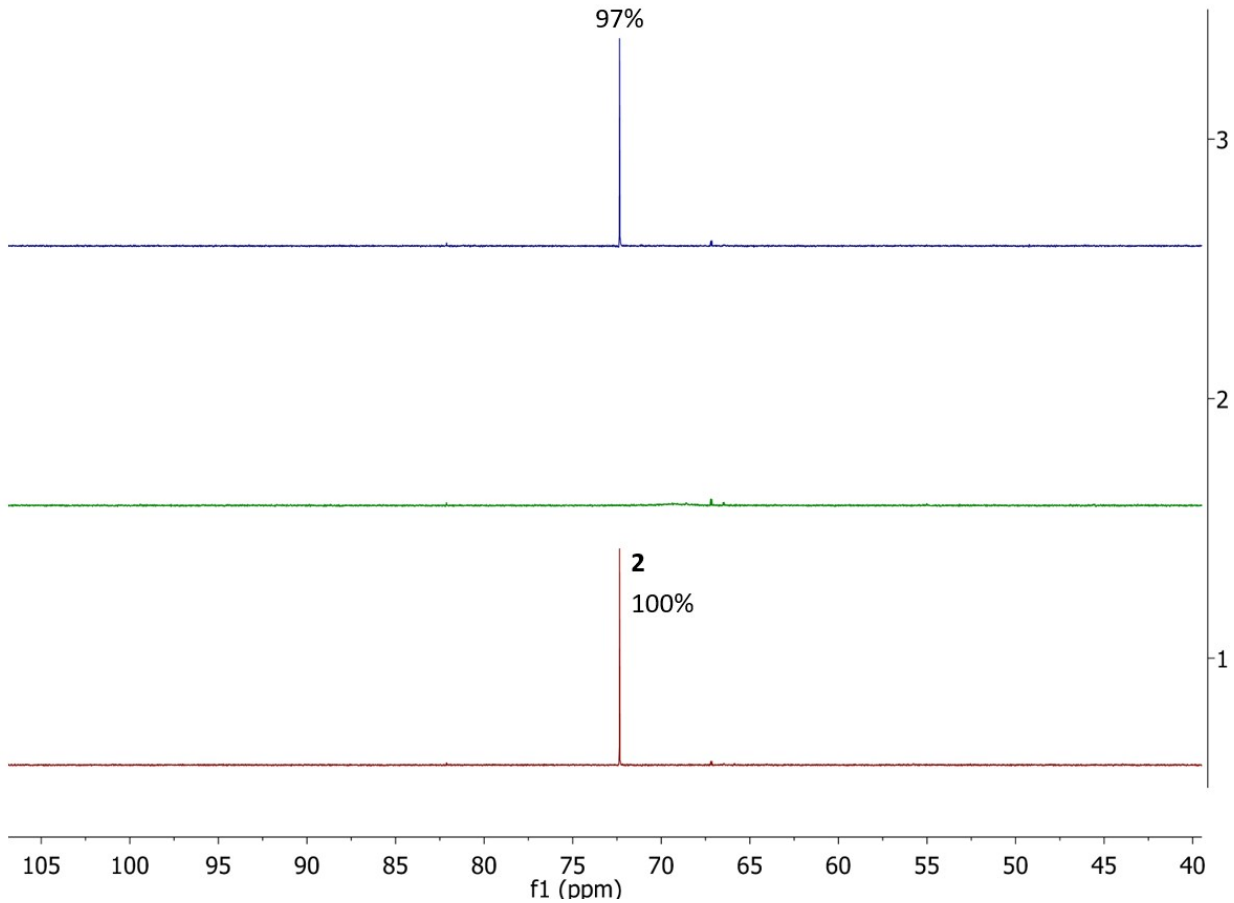

Bottom (1, maroon): 2.8 mg **2** (4.6 µmol) in THF-d_8. $^{31}P\{^{1}H\}$ NMR (202 MHz, THF-d_8, **2**): δ = 72.80 (s). *Middle (2, green)*: 2.8 mg **2** (4.6 µmol) with 1 eq. DMAH-BF_4 in THF-d_8. No phosphorus resonance is visible for the diamagnetic complex **2a** at 25 °C (see Fig. S9). *Top (3, blue)*: 2.8 mg **2** (4.6 µmol) with 1 eq. DMAH-BF_4 and 1.1 eq. DBU in THF-d_8. $^{31}P\{^{1}H\}$ NMR (202 MHz, THF-d_8): δ = 72.80 (s). **2** is reformed in 97% yield upon deprotonation of **2a** with DBU under N_2. Integrations are referenced to an internal standard of PMe_3 in a capillary tube.

Fig. S11: $^{31}P\{^{1}H\}$ NMR spectra showing deprotonation of **2a** with DBU under Ar

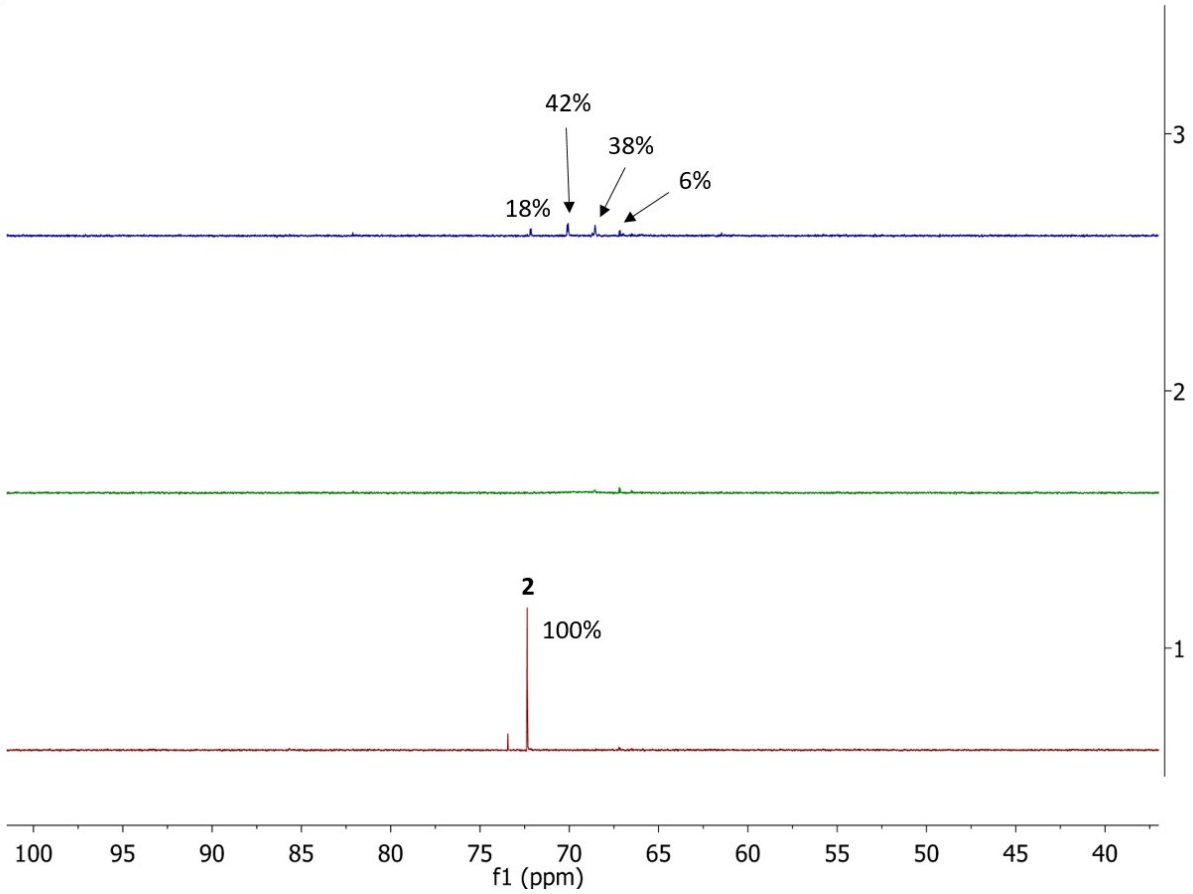

Bottom (1, maroon): 1.3 mg **2** (2.1 µmol) in THF-d_8. $^{31}P\{^{1}H\}$ NMR (202 MHz, THF-d_8, **2**): δ = 72.80 (s). *Middle (2, green)*: 1.3 mg **2** (2.1 µmol) with 1 eq. DMAH-BF_4 in THF-d_8. No phosphorus resonance is visible for the diamagnetic complex **2a** at 25 °C (see Fig. S9). *Top (3, blue)*: 1.3 mg **2** (2.1 µmol) with 1 eq. DMAH-BF_4 and 1.1 eq. DBU in THF-d_8. $^{31}P\{^{1}H\}$ NMR (202 MHz, THF-d_8): δ = 72.60 (d, *J* = 11.5 Hz, 18%), 70.53 (d, *J* = 11.1 Hz, 42%), 69.00 (br. s, 38%), 67.62 (d, *J* = 12.1 Hz, 6%). Upon deprotonation under Ar, a number of unidentified products are formed. In contrast to deprotonation under N_2 (Figure S10), no **2** is reformed, indicating that N_2 is lost upon protonation with DMAH-BF_4. Integrations are referenced to an internal standard of PMe_3 in a capillary tube.

Fig. S12: ^{1}H NMR spectrum showing formation of $[(PCP)Ir(H)(py)_x]^+$ from reaction of **2a** with pyridine-d_5

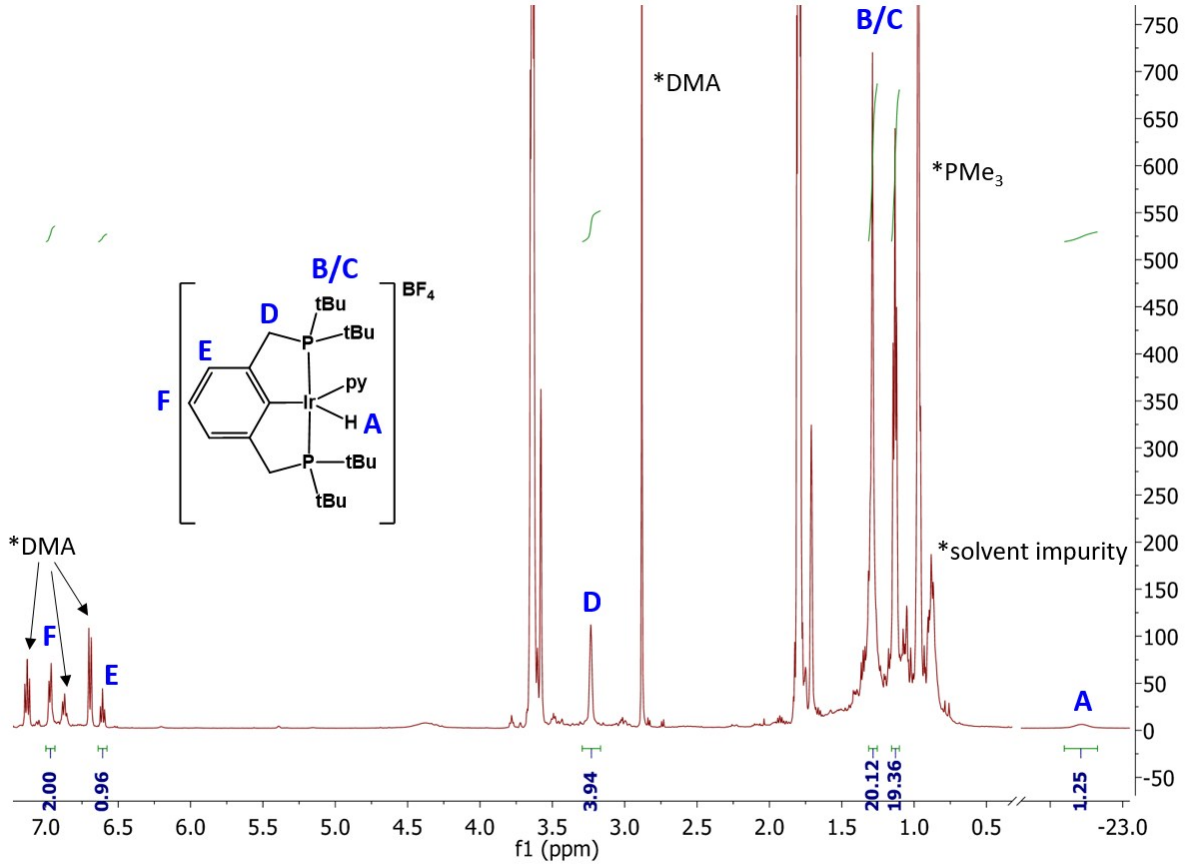

3.4 mg **2** (5.5 µmol) with 1 eq. DMAH-BF_4 added in THF-d_8, subsequently spiked with excess (one drop) pyridine-d_5. ^{1}H NMR (500 MHz, THF-d_8): δ = 6.91 (d, $^3J_{H,H}$ = 7.3 Hz, 2H, *m*-Ph), 6.55 (t, $^3J_{H,H}$ = 7.3 Hz, 1H, *p*-Ph), 3.17 (m, 4H, CH_2), 1.23 (m, 18H, C(CH_3)$_3$), 1.07 (m, 18H, C(CH_3)$_3$), -22.78 (br. s, 1H, Ir-*H*). While the number of bound pyridine molecules was not confirmed, the relatively downfield hydride resonance is characteristic of a weak donor bound *trans* to the hydride, suggesting a six-coordinate species in the presence of excess pyridine. This matches the reported ^{1}H NMR spectrum of $[(PCP)Ir(H)(THF)]^+$ in excess pyridine.[1] The PMe_3 peak is from the internal standard in a capillary tube.

Fig. S13: $^{31}P\{^{1}H\}$ NMR spectrum showing formation of $[(PCP)Ir(H)(py)_x]^+$ from reaction of **2a** with pyridine-d_5

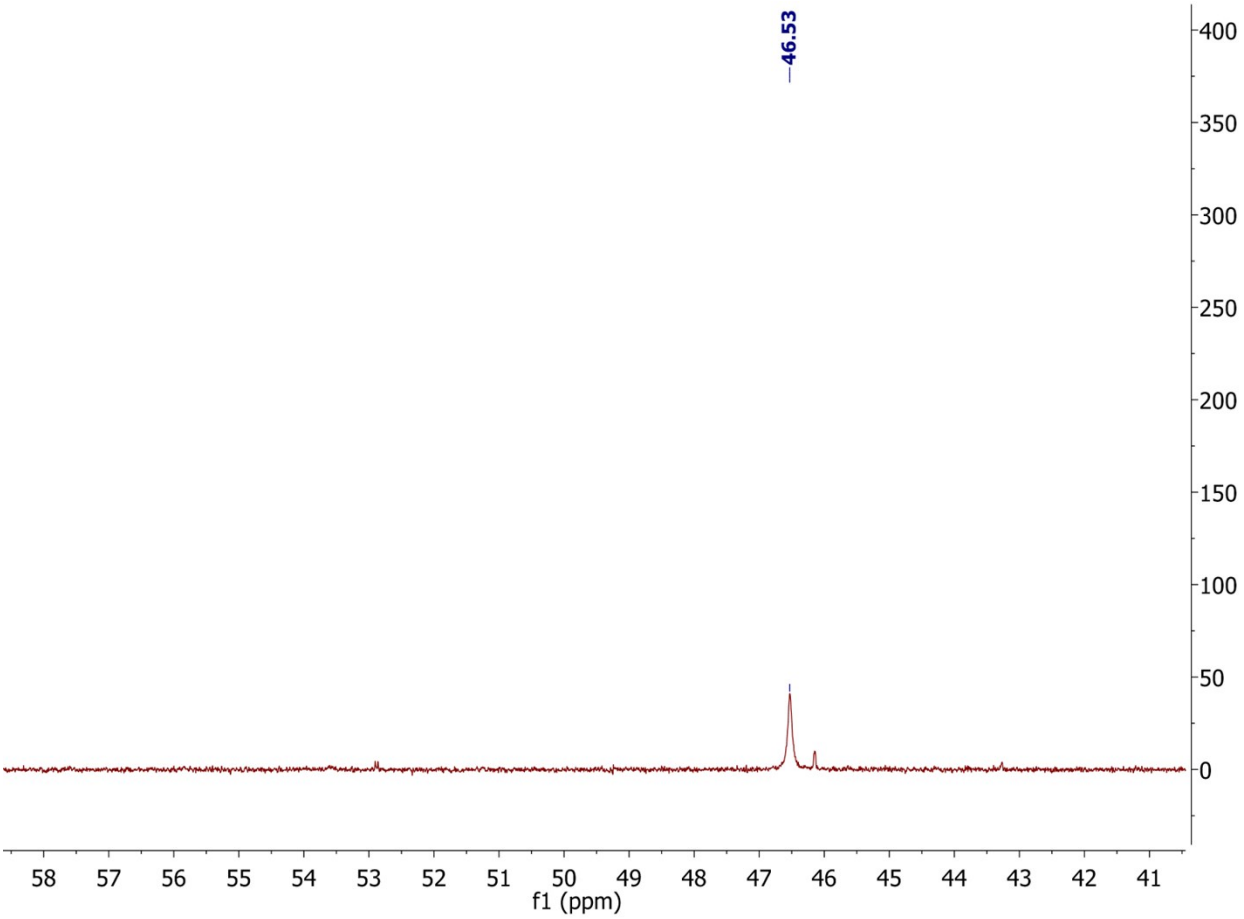

3.4 mg **2** (5.5 µmol) with 1 eq. DMA-BF_4 added in THF-d_8, subsequently spiked with excess (one drop) pyridine-d_5. $^{31}P\{^{1}H\}$ NMR (202 MHz, THF-d_8) δ = 46.53 (s). This matches the reported ^{31}P NMR spectrum of $[(PCP)Ir(H)(THF)]^+$ in excess pyridine.[1] Referenced to PMe_3 in a capillary tube.

Fig. S14: ATR-IR spectra of **2**, DMAH-BF_4, and **2a**

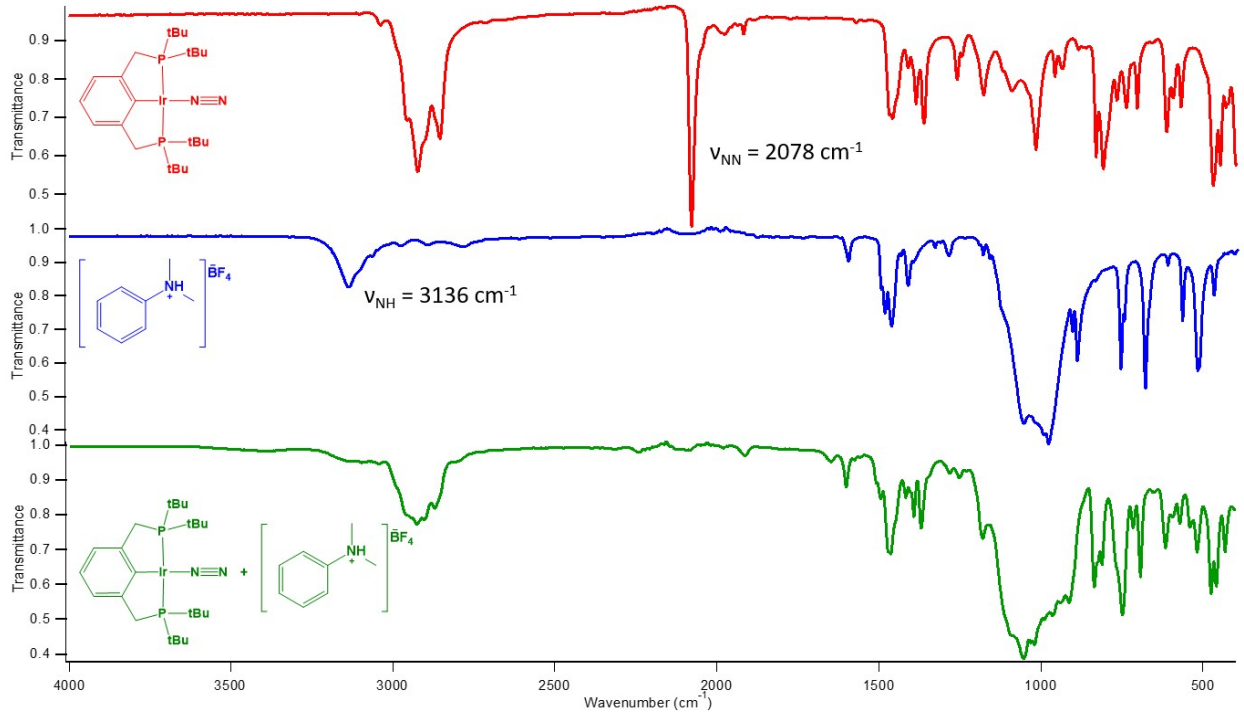

ATR-IR spectrum of **2** (*red, top*), DMAH-BF_4 (*blue, middle*), and after the addition of 1 eq. DMAH-BF_4 to 3.4 mg **2** (5.5 µmol) in THF-d_8 to form **2a** (*green, bottom*). The bottom spectrum was taken using the crude residue obtained after removing THF-d_8 under vacuum. The N-N stretch from **2** is no longer visible, indicating that **2a** does not contain N_2 in the solid state. Loss of the N-H stretch from DMAH-BF_4 confirms proton transfer from the anilinium to the metal complex occurred.

Fig. S15: CV of **1** in THF with added equiv TFA

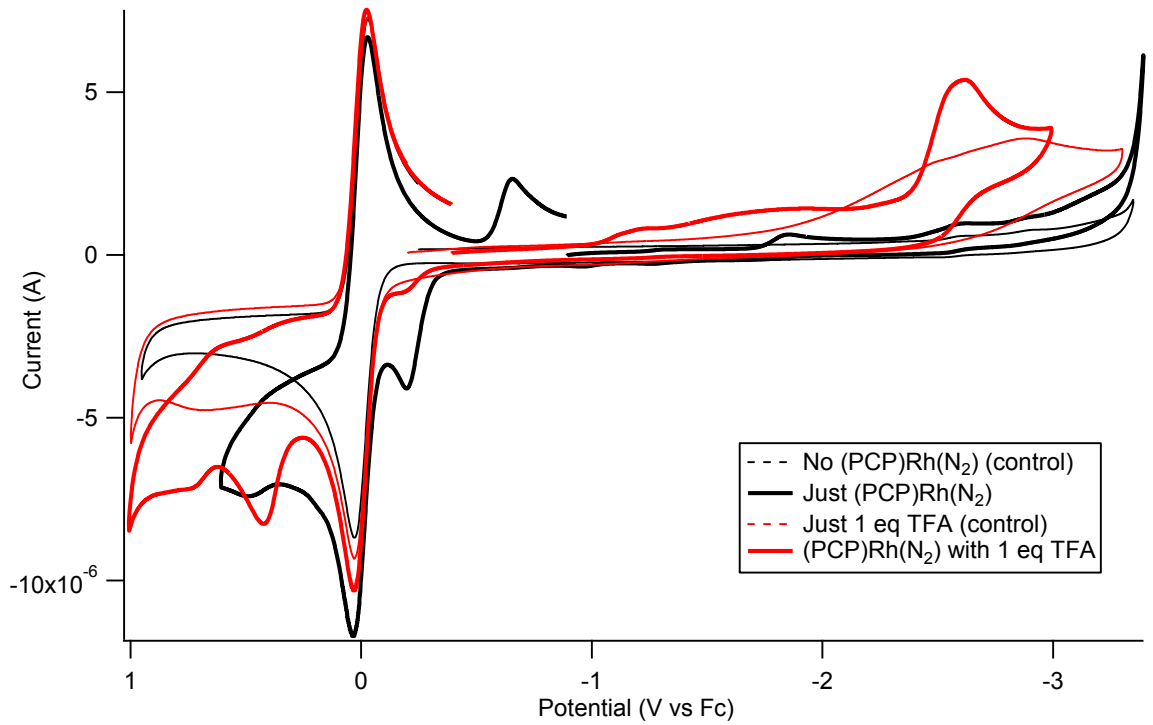

CV of 1.2 mg **1** in 5 mL THF (0.46 mM) with 0.1 M TBA-PF_6 and 1 eq. Fc added (black, solid) taken at 50 mV/s. Upon addition of 1 eq. TFA, an irreversible one-electron reduction occurs at -2.63 V vs. Fc (red, solid). IR compensation was set to 3200 Ω. Control experiments of 1 equiv Fc in THF with 0.1 M TBA-PF_6 without (black, dashed) and with (red, dashed) 1 eq. TFA confirm that this reduction event is dependent on the presence of both **1** and TFA.

Fig. S16: CV of **2** in THF with added equiv TFA

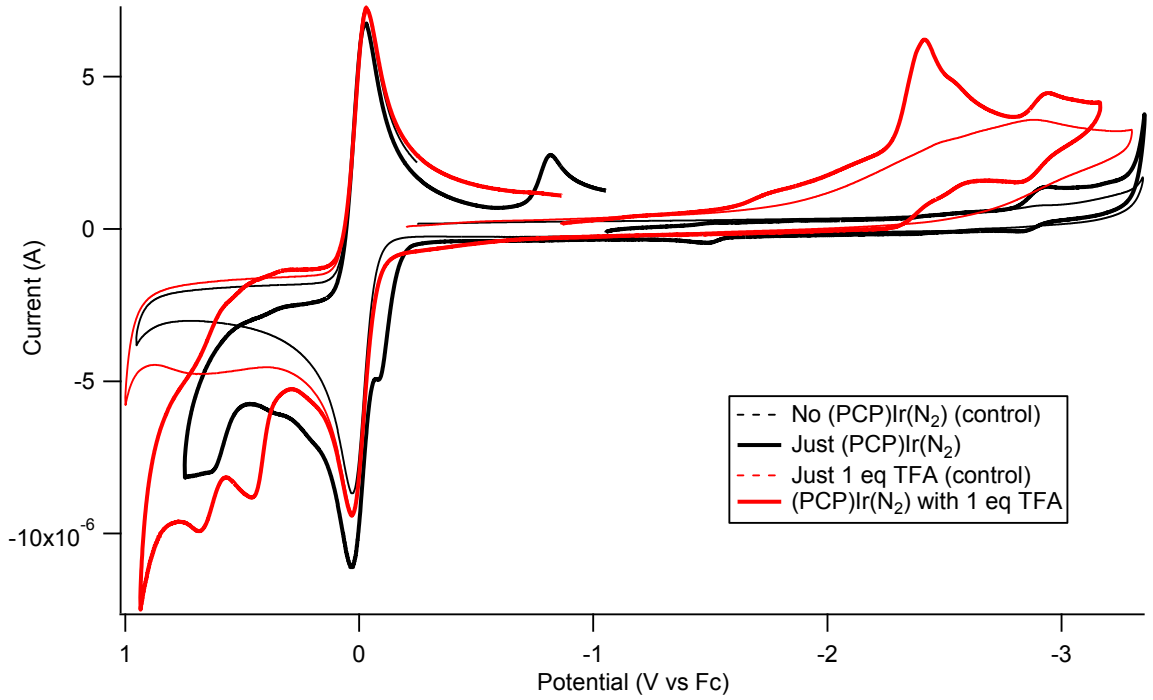

CV of 1.4 mg **2** in 5 mL THF (0.46 mM) with 0.1 M TBA-PF_6 and 1 eq. Fc added (black, solid) taken at 50 mV/s. Upon addition of 1 eq. TFA, an irreversible one-electron reduction occurs at -2.42 V vs. Fc (red, solid), followed by a substoichiometric reversible reduction at -2.88 V vs. Fc. IR compensation was set to 3200 Ω. Control experiments of 1 equiv Fc in THF with 0.1 M TBA-PF_6 without (black, dashed) and with (red, dashed) 1 equiv TFA confirm that these redox events are dependent on the presence of both **2** and TFA.

Fig. S17: CV of **1** in THF with large excess of TFA

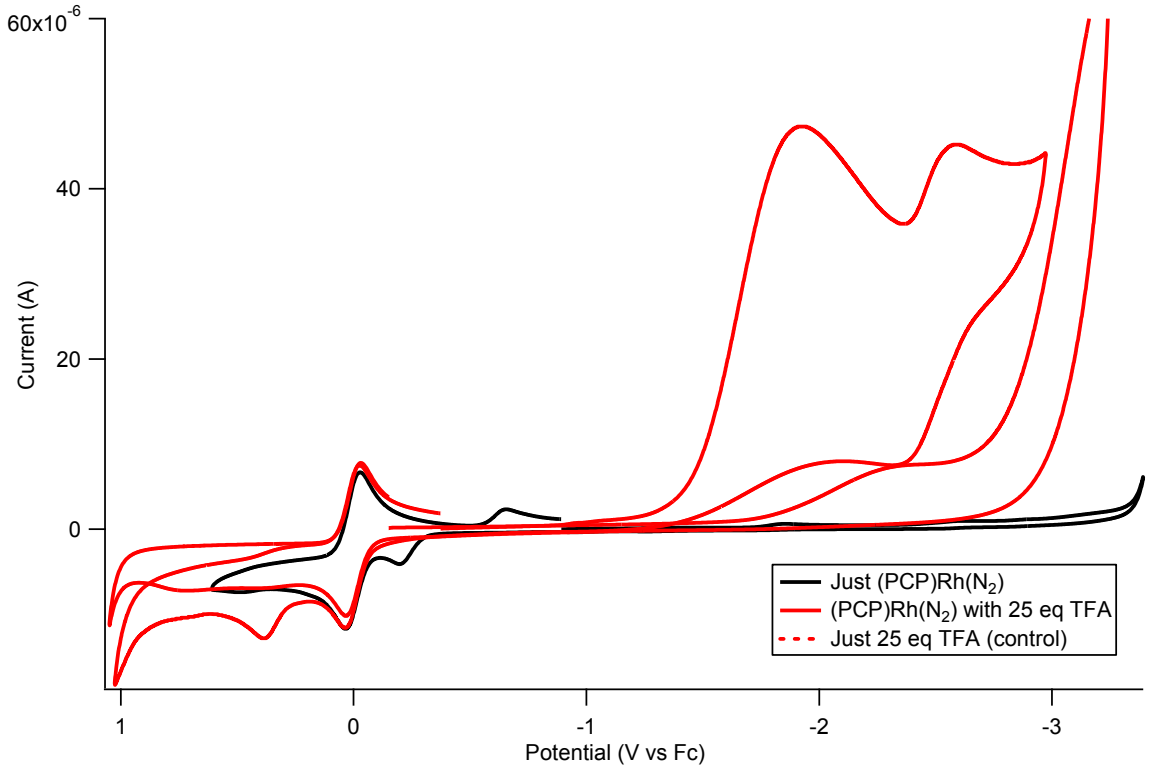

CV of 1.2 mg **1** in 5 mL THF (0.46 mM) with 0.1 M TBA-PF_6 and 1 eq. Fc added (*black, solid*) taken at 50 mV/s. Upon addition of 25 eq. TFA, a large irreversible reduction occurs with peak current at -1.93 V vs Fc (*red, solid*) followed by a second reduction at -2.59 V vs Fc. IR compensation was set to 3200 Ω. The large current of the first irreversible reduction upon flooding with acid (compare to 1 equiv TFA in Fig. S15) is characteristic of electrocatalytic proton reduction. Control experiments of 1 eq. Fc with 25 equiv TFA (*red, dashed*) confirm that the catalytic current is dependent on the presence of **1**.

Fig. S18: CV of **2** in THF with large excess of TFA

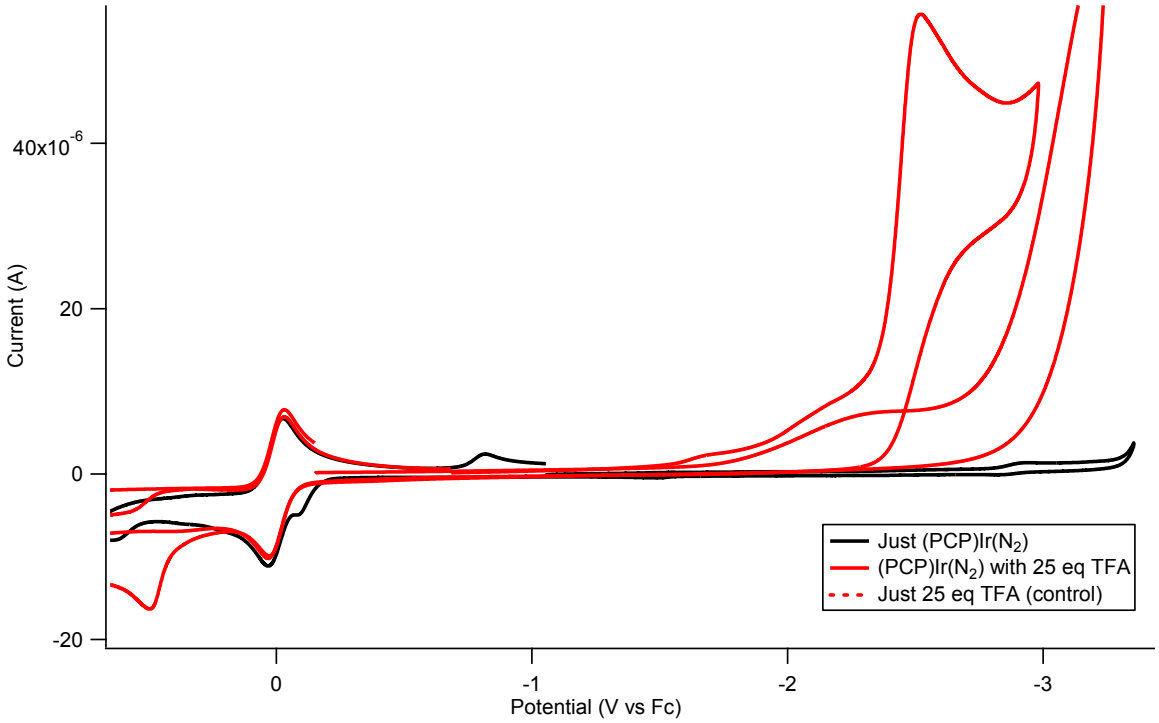

CV of 1.4 mg **2** in 5 mL THF (0.46 mM) with 0.1 M TBA-PF_6 and 1 eq. Fc added (*black, solid*) taken at 50 mV/s. Upon addition of 25 eq. TFA, a large irreversible reduction occurs with peak current at -2.53 V vs Fc (*red, solid*). IR compensation was set to 3200 Ω. The large current enhancement of this irreversible reduction upon flooding with acid (compare to 1 equiv TFA in Fig. S16) is characteristic of electrocatalytic proton reduction. Control experiments of 1 equiv Fc with 25 equiv TFA (*red, dashed*) confirm that the catalytic current is dependent on the presence of **2**.

Fig. S19: CV of **2** in THF with added DMAH-BF_4

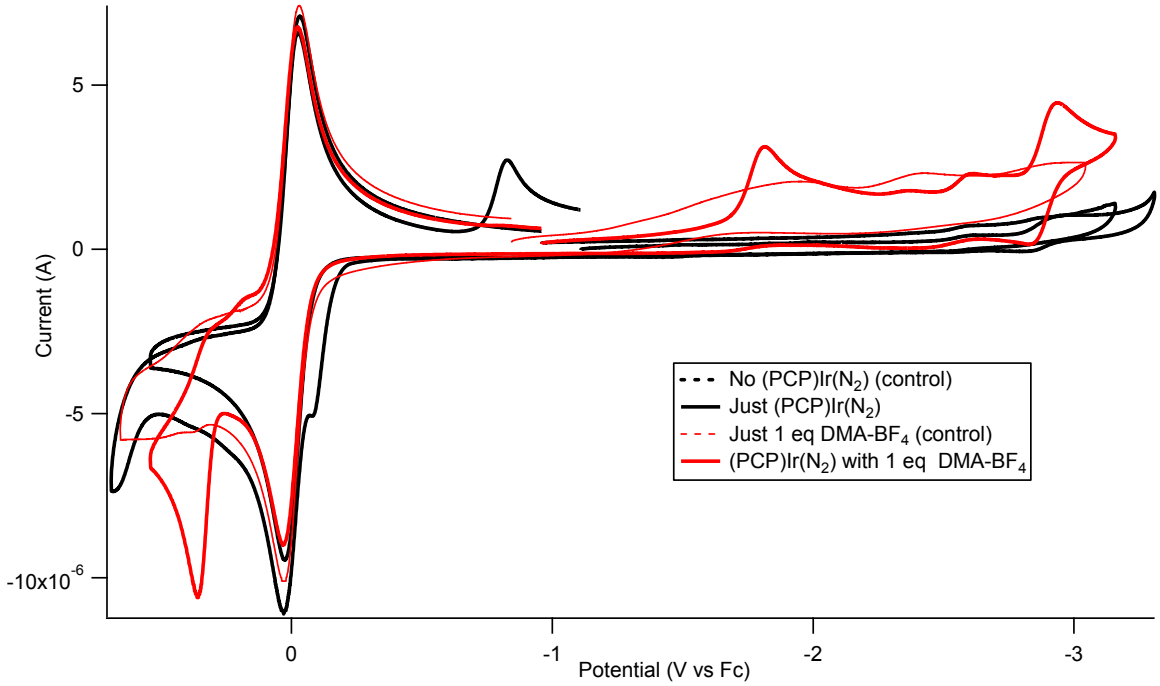

CV of 1.3 mg **2** in 5 mL THF (0.42 mM) with 0.1 M TBA-PF_6 and 1 equiv Fc added (black, solid) taken at 50 mV/s. Upon addition of 1 eq. DMAH-BF_4, an irreversible one-electron reduction occurs at -1.82 V vs. Fc (red, solid), followed by a reversible reduction at -2.89 V vs. Fc. IR compensation was set to 3000 Ω. Control experiments of 1 equiv Fc in THF with 0.1 M TBA-PF_6 without (black, dashed) and with (red, dashed) 1 equiv DMAH-BF_4 confirm that these redox events are dependent on the presence of both **2** and DMAH-BF_4.

Fig. S20: ^{1}H NMR spectra showing reduction of **2a** with $CoCp_2^*$

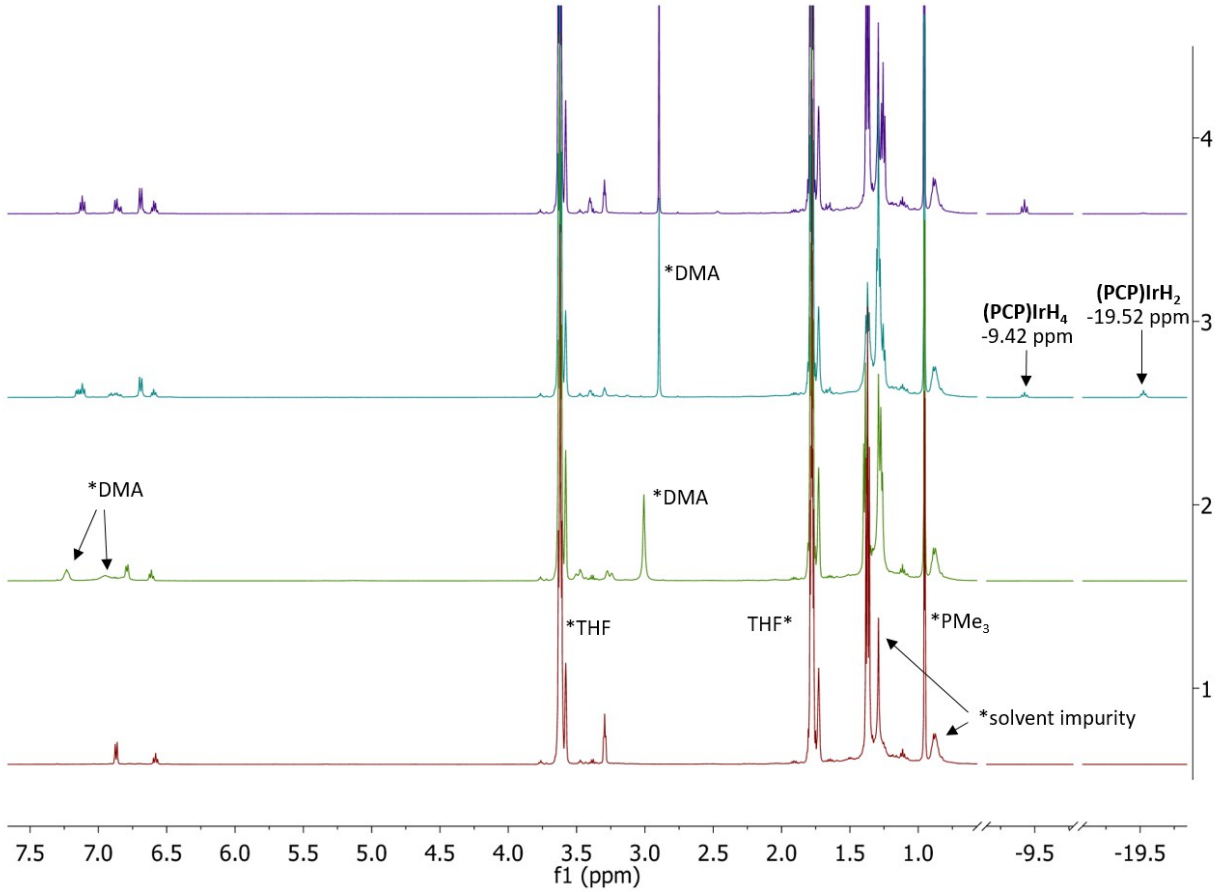

Bottom (1, maroon): 2.9 mg **2** (4.7 µmol) in THF-d_8. ^{1}H NMR (500 MHz, THF-d_8): δ = 6.83 (d, *J* = 7.4 Hz, 2H), 6.54 (t, *J* = 7.4 Hz, 1H), 3.25 (m, *J* = 3.9 Hz, 4H), 1.33 (m, *J* = 6.4 Hz, 36H). *Second (2, light green)*: 2.9 mg **2** with 1 eq. DMA-BF_4 added in THF-d_8 to form **2a**. *Third (3, blue-green)*: Reduction of **2a** with 1.1 eq. $CoCp_2^*$ in THF-d_8, showing hydride resonances at -9.42 ppm and -19.52 ppm characteristic of (PCP)IrH_4 and (PCP)IrH_2, respectively.[2, 3] Aromatic resonances at 6.83 ppm (d, *J* = 7.4 Hz) and 6.54 ppm (t, *J* = 7.4 H) correspond to **2**. *Top (4, purple)*: ^{1}H NMR spectrum after one week showing full conversion to **2** and (PCP)IrH_4. The PMe_3 peak is from the internal standard in a capillary tube.

Fig. S21: ^{1}H NMR spectrum of mixture of (PCP)IrH$_2$ and (PCP)IrH$_4$

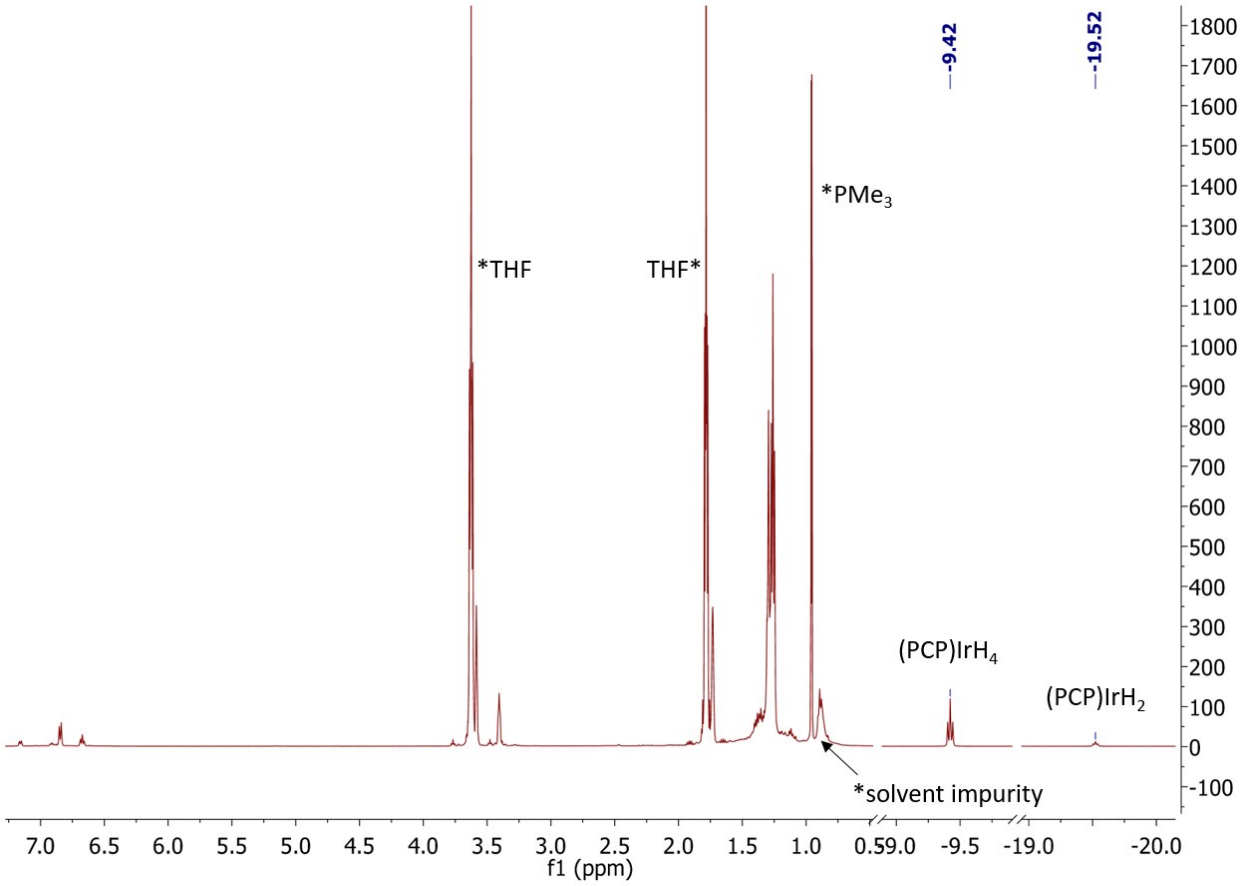

Mixture of (PCP)IrH$_2$[2] and (PCP)IrH$_4$[3] in THF-d_8, which were prepared according to literature procedures and match reported spectra. The PMe$_3$ peak is from the internal standard in a capillary tube.

Fig. S22: $^{31}P\{^{1}H\}$ NMR spectrum of mixture of $(PCP)IrH_2$ and $(PCP)IrH_4$

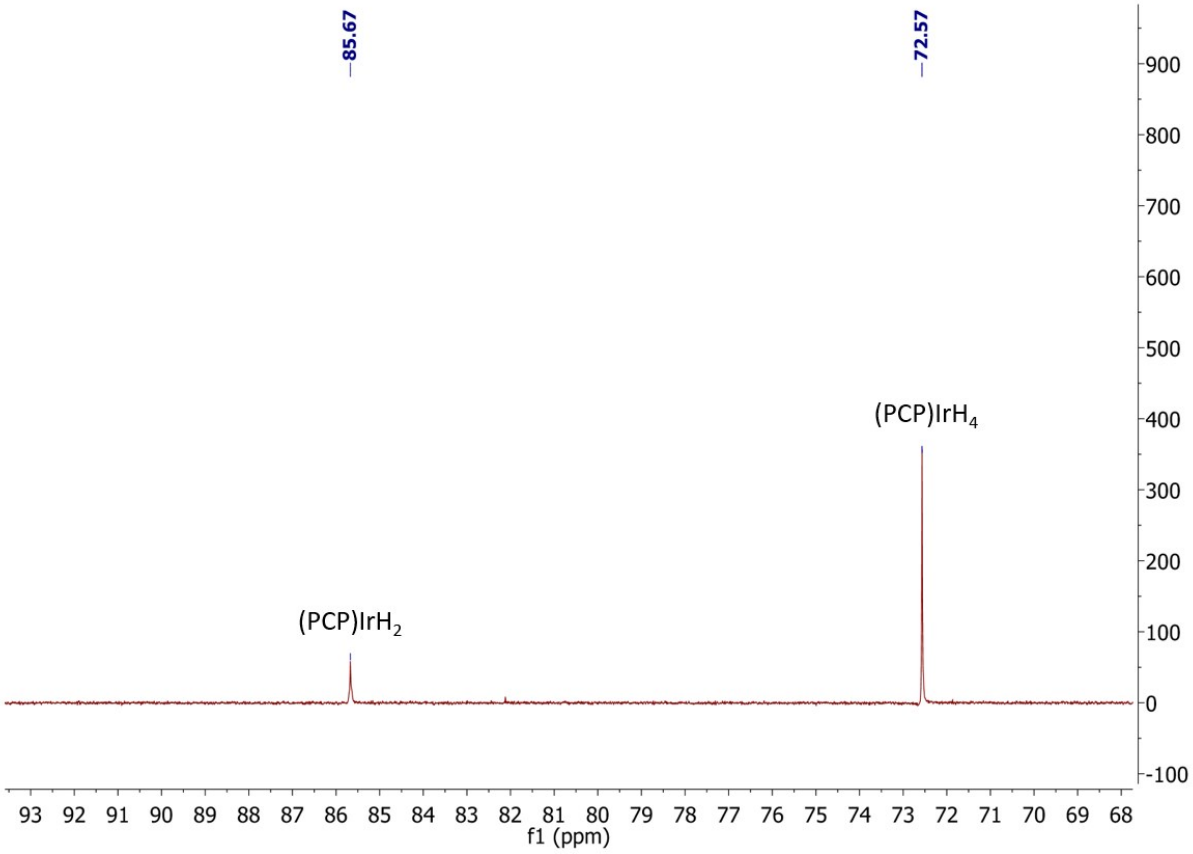

Mixture of $(PCP)IrH_2$ and $(PCP)IrH_4$ in THF-d_8, which were prepared according to literature procedures and match reported spectra. Referenced to PMe_3 in a capillary tube.

References:

1. A. G. Walden. “Oxidative Electrochemistry of Molecular Catalysts.” University of North Carolina at Chapel Hill, 2016.
2. M. Gupta, C. Hagen, R. J. Flesher, W. C. Kaska and C. M. Jensen, *Chem. Commun.*, 1996, **17**, 2083-2084.
3. T. J. Hebden, K. I. Goldberg, D. M. Heinekey, X. Zhang, T. J. Emge, A. S. Goldman and K. Krogh-Jespersen, *Inorg. Chem.*, 2010, **49**, 1733-1742.